

# Monopole Current Dynamics and Color Confinement

H. Ichie <sup>\*</sup>, H. Suganuma and A. Tanaka <sup>a</sup>

<sup>a</sup>Research Center for Nuclear Physics (RCNP), Osaka University  
Mihogaoka 10-1, Ibaraki, Osaka 567, Japan

Color confinement can be understood by the dual Higgs theory, where monopole condensation leads to the exclusion of the electric flux from the QCD vacuum. We study the role of the monopole for color confinement by investigating the monopole current system. When the self-energy of the monopole current is small enough, long and complicated monopole world-lines appear, which is a signal of monopole condensation. In the dense monopole system, the Wilson loop obeys the area-law, and the string tension and the monopole density have similar behavior as the function of the self-energy, which seems that monopole condensation leads to color confinement. On the long-distance physics, the monopole current system almost reproduces essential features of confinement properties in lattice QCD. In the short-distance physics, however, the monopole-current theory would become nonlocal and complicated due to the monopole size effect. This monopole size would provide a critical scale of QCD in terms of the dual Higgs mechanism.

## 1. QCD-monopole for Quark Confinement

Quantum Chromodynamics (QCD) is the fundamental theory of the strong interaction and describes not only hadrons but also their underlying structure in terms of quarks and gluons. In the high energy region, the QCD gauge coupling becomes small, and therefore the system can be described by the perturbative QCD, where quarks and gluons are good degrees of freedom. On the other hand, in the low energy region, there are various nontrivial phenomena like color confinement, dynamical chiral-symmetry breaking and topological defects due to the strong coupling nature of QCD. However, the essential degrees of freedom are unclear in the nonperturbative QCD, and their finding is strongly desired for understanding hadron physics.

In 1974, Nambu proposed an interesting idea that quark confinement can be interpreted using the dual version of the superconductivity[1]. In this picture, condensation of the color magnetic monopole is the key concept and leads to squeezing the color-electric flux between quarks through the dual Meissner effect. In 1981, 't Hooft showed that QCD is reduced into an abelian gauge field theory with magnetic monopoles after the abelian gauge fixing[2]. In this gauge, the only abelian gauge fields with monopoles would be essential for describing non-perturbative phenomena in the low energy region[3]-[9].

Recent lattice QCD simulations show strong evidence on this dual Higgs picture for the nonperturbative QCD in the Maximally Abelian (MA) gauge[6]-[9]. The MA gauge

---

<sup>\*</sup>ichie@rcnp.osaka-u.ac.jp

is considered as the best abelian gauge, and is realized by the gauge transformation so as to maximize the diagonal components of the gauge fields (or the link variables in the lattice formalism). In this gauge, information of the gauge configuration is concentrated into the diagonal components. According to the nontrivial homotopy class,  $\pi_2(\text{SU}(N_c)/\text{U}(1)^{N_c-1}) = Z_\infty^{N_c-1}$ [2], the QCD-monopole appears from the hedgehog-like configuration, which accompanies large fluctuation of the gauge field in the QCD vacuum. Since the classical monopole mass is in inverse proportion to the gauge coupling constant, monopoles can be easily excited in the low energy region with the large gauge coupling. Therefore, QCD-monopoles are expected to be the relevant degrees of freedom for the description of the non-perturbative QCD. However, such a picture for the confinement mechanism in terms of monopole condensation can be applied only in the infrared region. In the ultraviolet region, the large monopole mass leads to suppression of the monopole excitation, and the QCD system seems to be trivial in terms of topology.

In the dual Higgs phase, only short-range interactions remain among monopoles, and therefore the monopole current dynamics is subjected to a simple action. Thus, the nonperturbative QCD would be described only by the monopole degrees of freedom. In this paper, we study the monopole current dynamics and color confinement from the idealized monopole-current action.

## 2. Monopole Current Dynamics and Kosterlitz-Thouless Type Transition

We study the monopole current system using the idealized monopole action, and investigate the role of the monopole currents for color confinement. In general, the current action includes nonlocal interaction terms. In the confinement phase, however, the nonlocal part of the interaction can be neglected, because the currents are expected to interact each other only in the short distance due to the *screening effect* by the dual Higgs mechanism[3]. With the current conservation, the partition functional is written as

$$Z = \int Dk_\mu \exp\{-\alpha \int d^4x \text{tr} k_\mu^2(x)\} \delta(\partial_\mu k_\mu), \quad (1)$$

where  $k_\mu(x) \equiv k_\mu^3(x) \cdot \tau^3/2$  and  $\alpha$  are the monopole current and energy for the unit current length, respectively. In order to perform the path integral (1), we put the system on the 4-dimensional lattice with the lattice spacing  $a$ . In the lattice formalism, the monopole currents are defined on the dual lattice,  $k_\mu^{\text{lat}}(s) \equiv e/(4\pi) \cdot a^3 k_\mu^3(s)$ . The partition function is given as  $Z = \sum_{k_\mu^{\text{lat}}} \exp\{-\alpha^{\text{lat}} \sum_s k_\mu^{\text{lat}}(s)^2\} \delta(\partial_\mu k_\mu^{\text{lat}}(s))$ , where  $\alpha^{\text{lat}} \equiv \alpha/2 \cdot (4\pi/ea)^2$ .

The lattice QCD simulation shows that one long monopole loop and many short loops appear in the confinement phase. The only long loop becomes important for the properties of the vacuum, while many short loops are originated from the fluctuation in the ultraviolet region and therefore can be neglected. In this system, the partition function can be approximated as the single monopole loop ensemble with the length  $L$ ,  $Z = \sum_L \rho(L) e^{-\alpha L}$ , where  $L$  and  $\rho(L)$  are length of the monopole loop and its configuration number, respectively. The monopole current with length  $L$  is regarded as the  $L$  step self-avoiding random walk, where  $2d - 1 = 7$  direction is possible in each step. Therefore,  $\rho(L)$  is roughly estimated as  $(2d - 1)^L = 7^L$ . Using this partition function, the expectation value of the

monopole current length is found to be

$$\langle L \rangle = \frac{1}{Z} \sum_L \rho(L) L e^{-\alpha L} = \begin{cases} \{\alpha - \ln(2d - 1)\}^{-1} & \text{if } \alpha > \ln(2d - 1) \\ \infty & \text{if } \alpha < \ln(2d - 1). \end{cases} \quad (2)$$

When the energy  $\alpha$  is larger than the entropy  $\ln(2d - 1)$ , the monopole loop length is finite. However, when  $\alpha$  is smaller than the entropy, the monopole loop length becomes infinite, which is a signal of monopole condensation in the current representation.

In performing the simulation, we construct the monopole current as the sum of plaquettes of the monopole current because of the current conservation condition. First, we prepare a random monopole current system (hot start) and no monopole current system (cold start). Then, we update the *link* of the monopole current using the Metropolis method.

We generate the monopole current system on  $8^4$  lattices. Fig.1 shows the monopole current vacuum for the typical cases, ( $\alpha = 1.5, 1.8, 1.9$ ) at a fixed time. Corresponding to each case, we show in Fig.2 the histograms of the monopole loop length[10] of one cluster with 40 configurations. For large  $\alpha$ , only small loops appear and their density is small. On the other hand, for small  $\alpha$ , there appear one long monopole loop and some short loops, and the monopole currents are complicated and dense. Between these two regions, there is critical value,  $\alpha_c \simeq 1.8$ , where monopole loops with various length appear. The monopole density  $\rho_M \equiv \frac{1}{4V} \sum_{s,\mu} |k_\mu(s)|$  and the clustering parameter  $\eta \equiv \frac{\sum_i L_i^2}{(\sum_i L_i)^2}$  are shown in Fig.3. and Fig.4, respectively. Here,  $L_i$  is the loop length of the  $i$ -th monopole cluster. The property of the clustering parameter is that it goes to unity when many loops cluster and unite to one long loop, and it approaches to zero when loops never cluster each other. When  $\alpha$  becomes small, the monopole density becomes large gradually at  $\alpha \lesssim \alpha_c$ . However, the clustering parameter is drastically changed at  $\alpha_c$ . Quantitatively, the critical value of monopole current energy,  $\alpha_c \simeq 1.8$ , is close to  $\ln 7 \simeq 1.95$ , which is corresponding to the entropy for the 1 step self-avoiding random walk. This vacuum can be roughly approximated with the vacuum made of the longest monopole loop alone in terms of the mechanism of the transition. Such a transition is quite similar to the Kosterlitz-Thouless type transition in 2-dimensional superconductors, where vortex condensation may occur.

### 3. Dual Field Formalism and Role of Monopoles for Confinement

In this section, we study how these monopole currents contribute to the color confinement properties. Quark confinement is characterized by the linear inter-quark potential, which can be obtained from the area-law behavior of the Wilson loop,  $\langle W \rangle = \langle P \exp(i e \oint A_\mu dx_\mu) \rangle$ . Therefore, it is desired to extract the gauge variable from the monopole current  $k_\mu$ . We now derive the abelian gauge variable in stead of the non-abelian gauge field, because the lattice QCD results show the color confinement phenomena can be discussed only with abelian part to some extent. However, in the presence of the magnetic monopoles, the ordinary abelian gauge field  $A_\mu(x)$  inevitably includes the singularity as the Dirac string, which leads to some difficulties in the field theoretical treatment. Instead, the dual field formalism is much useful to describe the monopole current system, because the dual gauge field  $B_\mu(x)$  can be introduced without the singularity

for such a system with  $k_\mu \neq 0$  and  $j_\mu = 0$ . This is the dual version of the ordinary gauge theory with  $A_\mu(x)$  for the QED system with  $j_\mu \neq 0$  and  $k_\mu = 0$ .

Let us consider the derivation of the dual gauge field  $B_\mu(x)$  from the monopole current  $k_\mu(x)$ . Using the relation  $\partial_\mu {}^*F_{\mu\nu} = k_\nu$  with  ${}^*F_{\mu\nu} \equiv \frac{1}{2}\epsilon_{\mu\nu\alpha\beta}F_{\alpha\beta}$ ,  ${}^*F_{\mu\nu}$  is given by the 2-form of the dual gauge field  $B_\mu$  as  ${}^*F_{\mu\nu} = \partial_\mu B_\nu - \partial_\nu B_\mu$ , so that one finds  $\partial^2 B_\nu - \partial_\nu(\partial_\mu B_\mu) = k_\nu$ . By taking the dual Landau gauge,  $\partial_\mu B_\mu = 0$ , this field equation becomes quite a simple form,  $\partial^2 B_\mu = k_\mu$ . Therefore, starting from the monopole current configuration  $k_\mu(x)$ , we derive the dual gauge field  $B_\mu$ ,

$$B_\mu(x) = \partial^{-2}k_\mu(x) = -\frac{1}{4\pi^2} \int d^4y \frac{k_\mu(y)}{|x-y|^2}. \quad (3)$$

Using the dual gauge field, the Wilson loop is obtained as  $\langle W \rangle = \langle \exp\{ie \oint A_\mu dx_\mu\} \rangle = \langle \exp\{ie \frac{1}{2}\epsilon_{\mu\nu\alpha\beta} \int d\sigma_{\mu\nu} {}^*F_{\alpha\beta}\} \rangle = \langle \exp\{ie \frac{1}{2}\epsilon_{\mu\nu\alpha\beta} \int d\sigma_{\mu\nu}(\partial_\alpha B_\beta - \partial_\beta B_\alpha)\} \rangle$ .

Now, we apply this dual field formalism to the monopole current system discussed in Section 2. Since the monopole current  $k_\mu^{\text{lat}}(s)$  is generated on the lattice with the mesh  $a$ , the continuous dual field  $B_\mu(x)$  is derived from  $k_\mu(x) \equiv 4\pi/e \cdot k_\mu^{\text{lat}}(s)\delta^3(x-s)$  using Eq.(3), in principle. In estimating the integral in Eq.(3) numerically, we use a fine lattice with a small mesh  $c$ . *To extract  $B_\mu(x)$  correctly, the mesh  $c$  is to be taken enough small.* However, too fine mesh is not necessary because the original current  $k_\mu^{\text{lat}}(s)$  includes the error in the order of  $a$ . Numerical analyses show that the use of  $c \simeq a$  is too crude for the correct estimation of the integral in Eq.(3). Instead, the calculation with  $c \leq a/2$  is good enough for the estimation of  $B_\mu(x)$ , and hence we take  $c = a/2$  hereafter. On lattices, the dual gauge field  $\theta_\mu^{\text{dual}} \equiv aeB_\mu/2$  is defined in the dual Landau gauge,  $\theta_\mu^{\text{dual}}(s+\mu) \equiv 2\pi \sum_{s'} \Delta(s-s')k_\mu^{\text{lat}}(s')$ , using the lattice Coulomb propagator  $\Delta(s) = (\partial_\mu \partial'_\mu)^{-1}$ , where  $\partial'$  denotes the backward derivative. The dual version of the abelian field strength  $\theta_{\mu\nu}^{\text{dual}} \equiv ea^2 {}^*F_{\mu\nu}/2$  is defined by  $\theta_{\mu\nu}^{\text{dual}}(s) \equiv \partial'_\mu \theta_\nu^{\text{dual}}(s) - \partial'_\nu \theta_\mu^{\text{dual}}(s)$ .

The expectation value of the Wilson loop  $\langle W \rangle$  is shown in Fig.5. The Wilson loop exhibits the area-law and the linear confinement potential:  $\ln\langle W \rangle$  decreases linearly with the inter-quark distance, where its slope corresponds to the string tension. Quantitatively, the string tension is measured by the Creutz ratio, and we show in Fig.6  $\chi(3,3)$  as a typical example. For  $\alpha < \alpha_c$ , the string tension decreases as  $\alpha$  increases, and its behavior is similar to the lattice QCD result by setting  $\alpha = 0.8\beta$ . For  $\alpha > \alpha_c$ , the string tension becomes almost vanishes. It is worth mentioning that the behavior of string tension or the Creutz ratio becomes similarly to the monopole density shown in Fig.3. Thus, the confinement force is controlled by the monopole density, and therefore monopoles can be regarded as the essential degrees of freedom for color confinement.

#### 4. Monopole Size and Critical Scale in QCD

In the final section, we compare the monopole current system with abelian projected QCD [6,7] especially in terms of the coupling correspondence and the size of QCD-monopoles.

To begin with, let us consider one magnetic monopole with an intrinsic radius  $R$  in the multi-monopole system. In the static frame of the monopole, it creates a spherical magnetic field,  $\mathbf{H}(r) = \frac{g(r)}{4\pi r^3} \mathbf{r} = \frac{\mathbf{r}}{e(r)r^3}$  for  $r \geq R$  and  $\mathbf{H}(r) = \frac{g(r)}{4\pi R^3} \mathbf{r} = \frac{\mathbf{r}}{e(r)R^3}$  for  $r \leq R$ ,

where the QCD running gauge coupling  $e(r)$  is used to include the vacuum polarization effect. Here, the effective magnetic-charge distribution is assumed to be constant inside the monopole for the simplicity.

Now, we consider the lattice formalism with a large mesh  $a > R$ . The electromagnetic energy observed on the lattice around a monopole is roughly estimated as

$$M(a) \simeq \int_a^\infty d^3x \frac{1}{2} \mathbf{H}(r)^2 \simeq \frac{g^2(a)}{8\pi a} = \frac{2\pi}{e^2(a)a}, \quad (4)$$

which is largely changed depending on the lattice mesh  $a$ . This simple estimation neglects the possible reduction of  $g(r)$  in the infrared region due to the asymptotic freedom of QCD. The screening effect of the magnetic field by other monopoles also reduces  $g(r)$  effectively in a dense monopole system. However,  $M(a)$  is modified by at most factor 2 ( $M(a) = \frac{\pi}{e^2(a)a}$ ) even for the screening case as  $g(r) = g(a) \cdot \theta(2a - r)$ . Then, even in the multi-monopole system,  $M(a)$  would provide an approximate value for the electromagnetic energy on lattices created by one monopole, and we call  $M(a)$  as ‘lattice monopole mass’.

For the large mesh  $a > R$ , the monopole contribution to the lattice action reads  $S = M(a)a \cdot L$ , where  $L$  denotes the length of the monopole current measured in the lattice unit  $a$ . Therefore,  $M(a)$  is closely related to the monopole-current coupling  $\alpha^{\text{lat}}$  and  $\beta = 2N_c/e^2$ ,  $\alpha^{\text{lat}} \simeq M(a)a \simeq \frac{2\pi}{e^2(a)} = \frac{\pi}{2} \cdot \beta_{\text{SU}(2)}$ . For the above screening case, this relation becomes  $\alpha^{\text{lat}} \simeq M(a)a \simeq \frac{\pi}{e^2(a)} = \frac{\pi}{4} \cdot \beta_{\text{SU}(2)}$ , which is consistent with the numerical result,  $\alpha = 0.8\beta$ , discussed in Section 3. Here, as long as the mesh is large as  $a > R$ , the lattice monopole action would not need modification by the monopole size effect, and the current coupling  $\alpha^{\text{lat}}$  is proportional to  $\beta$ . Quantum mechanically, there is the energy fluctuation about  $a^{-1}$  at the scale  $a$ , and therefore monopole excitation occurs very often at the long-distance scale satisfying  $M(a) \lesssim a^{-1}$ . Thus,  $M(a)a \simeq \alpha^{\text{lat}}$  is the control parameter for the monopole excitation at the scale  $a(> R)$ , and we can obtain the quantitative criterion for ‘monopole condensation’ as  $M(a)a \lesssim \ln(2d - 1)$  from the analysis using the current dynamics in Section 2.

Second, we discuss the ultraviolet region with  $a < R$ . In the current dynamics, there exists a critical coupling  $\alpha_c \simeq \ln(2d - 1)$  as shown in Section 2 and 3. Above  $\alpha_c$ , the lattice current action provides no monopole condensation and no confinement, while  $\beta \rightarrow \infty$  can be taken in the original QCD keeping the confinement property shown in Fig. 6. Such a discrepancy between  $\beta$  and  $\alpha$  can be naturally interpreted by introducing the monopole size effect. Obviously, the monopole-current theory should be drastically changed in the ultraviolet region as  $a < R$ , if the QCD-monopole has its peculiar size  $R$ .

Here, let us reconsider the relation between  $a$  and  $\alpha^{\text{lat}}$  in the lattice current action. Similarly in the lattice QCD, the action has no definite scale except for the lattice mesh  $a(> R)$ , and therefore the scale unit  $a$  would be determined so as to reproduce a suitable dimensional variable, e.g. the string tension  $\sigma \simeq 1\text{GeV}/\text{fm}$ , in the monopole current dynamics. For instance,  $a$  is determined as a function of  $\alpha^{\text{lat}}$  using the Creutz ratio  $\chi \simeq \sigma a^2$  in Fig.6. Therefore,  $a$  should reach  $R$  before realizing  $\alpha^{\text{lat}} \rightarrow \alpha_c^{\text{lat}}$ , and the framework of the current theory is to be largely modified due to the monopole size effect for  $a < R$ .

Finally, we consider the fine lattice with a small mesh  $a < R$ , and study the monopole size effect to the current action (1). In this case, the extended structure of the QCD-

monopole is observed on the lattice, and the monopole creates the electromagnetic energy

$$M(a) \simeq \int_a^\infty d^3x \frac{1}{2} \mathbf{H}(r)^2 \simeq \frac{g^2(R)}{8\pi R} + \int_a^R dr r^4 \frac{g^2(r)}{8\pi R^6} \simeq \frac{g^2(R)}{8\pi R} = \frac{2\pi}{e^2(R)R} \quad (5)$$

on the lattice. Then, the ‘lattice monopole mass’  $M(a)$  is determined mainly by the size  $R$ , and is almost  $a$ -independent. Accordingly, the lattice action should be changed as

$$S = M(R)a \sum_{(s,s'),\mu} k_\mu(s)k_\mu(s') \cdot \theta\left(\frac{R}{a} - |s - s'|\right) \delta_{s_\mu,s'_\mu} \quad (6)$$

because of the self-avoidness originating from the monopole size  $R$ . Thus, the monopole-current theory becomes nonlocal in the ultraviolet region  $a < R$ .

In conclusion, the QCD-monopole size  $R$  provides a critical scale for the description of QCD in terms of the dual Higgs mechanism. In the infrared region as  $a > R$ , QCD can be approximated as a local monopole-current action[3], and the QCD vacuum can be regarded as the dual superconductor. On the other hand, in the ultraviolet region as  $a < R$ , the monopole theory becomes nonlocal and complicated due to the monopole size effect, and the perturbative QCD would be applicable instead.

We acknowledge Prof. H. Toki, Dr. A. Hosaka and Prof. Z. Ma for their kind encouragement. One of authors (H.I.) is supported by Research Fellowships of the Japan Society for the Promotion of Science for Young Scientists.

## REFERENCES

1. Y. Nambu, Phys. Rev. **D10** (1974) 4262.
2. G. 't Hooft, Nucl. Phys. **B190** (1981) 455.
3. Z. F. Ezawa and A. Iwazaki, Phys. Rev. **D25** (1982) 2681 ; **D26** (1982) 631.
4. H. Suganuma, H. Toki, S. Sasaki, H. Ichie, Prog. Theor. Phys. (Suppl.) **120** ('95) 57.  
H. Suganuma, S. Sasaki and H. Toki, Nucl. Phys. **B435** (1995) 207.
5. H. Ichie, H. Suganuma and H. Toki, Phys. Rev. **D52** (1995) 2994; **D54** (1996) 3382.
6. A. Di Giacomo, Nucl. Phys. **B** (Proc.Suppl.) **47** (1996) 136 and references therein.
7. M. I. Polikarpov, Nucl. Phys. **B** (Proc.Suppl.) **53** (1997) 134 and references therein.
8. O. Miyamura, Phys. Lett. **B353** (1995) 91; Nucl. Phys. **B** (Proc.Suppl.) **42** ('95) 538.
9. H.Suganuma, A.Tanaka, S.Sasaki and O.Miyamura, Nucl. Phys.**B** (PS) **47** ('96) 302.
10. A. Bode, T. Lipper and K. Schilling, Nucl. Phys. **B** (Proc. Suppl.) **34** (1994) 549.
11. H. Ichie and H. Suganuma, Proc. of INSAM Symp. '96, Hiroshima, INSAM report.

## Figure Captions

**Fig.1** The monopole currents for typical cases, (a)  $\alpha = 1.9$ , (b)  $\alpha = 1.8$ , (c)  $\alpha = 1.5$ .

**Fig.2** The histograms of the monopole current length of each cluster with 40 configurations for the same cases with Fig.1.

**Fig.3** The monopole density  $\rho_M$  as the function of  $\alpha$ . The monopole density becomes small for large  $\alpha$  and almost vanishes for  $\alpha > \alpha_c$ .

**Fig.4** The clustering parameter  $\eta$  as the function of  $\alpha$ . At  $\alpha_c$ ,  $\eta$  is drastically changed.

**Fig.5** The expectation value of the Wilson loop  $\langle W(I \times J) \rangle$  on fine mesh  $c = a/2$  for  $\alpha = 1.7, 1.8, 1.9$ . The area-law behavior indicates the linear interquark potential.

**Fig.6** The Creutz ratio as the function of  $\alpha$  in the multi-monopole system. The dotted line denotes the Creutz ratio as the function of  $\alpha = 0.8\beta$  in the lattice QCD.

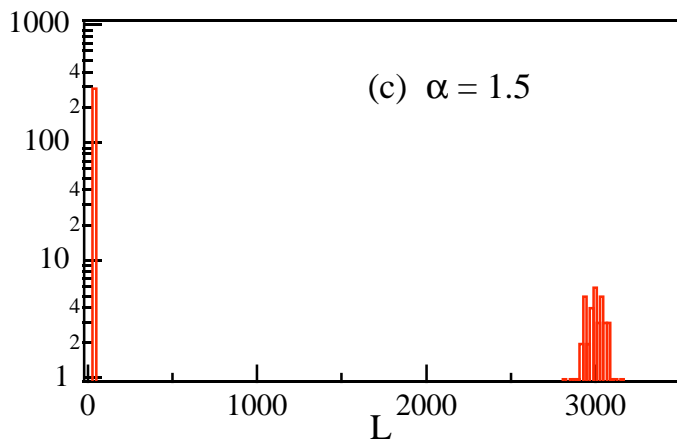
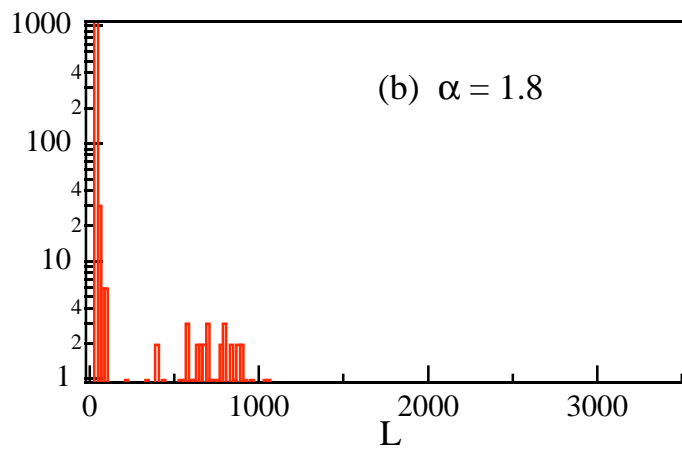
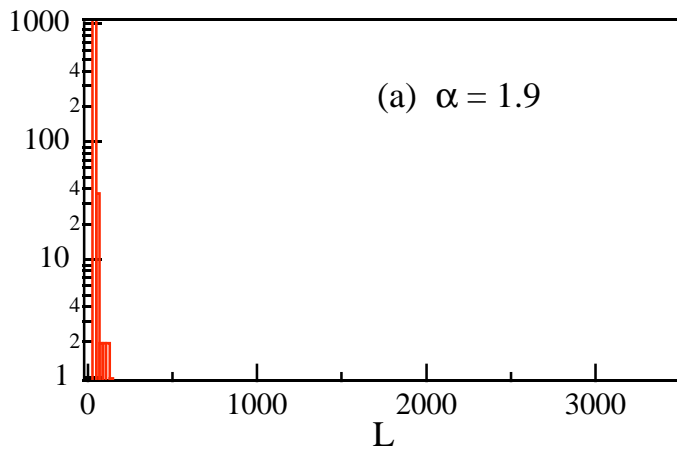


Fig.2

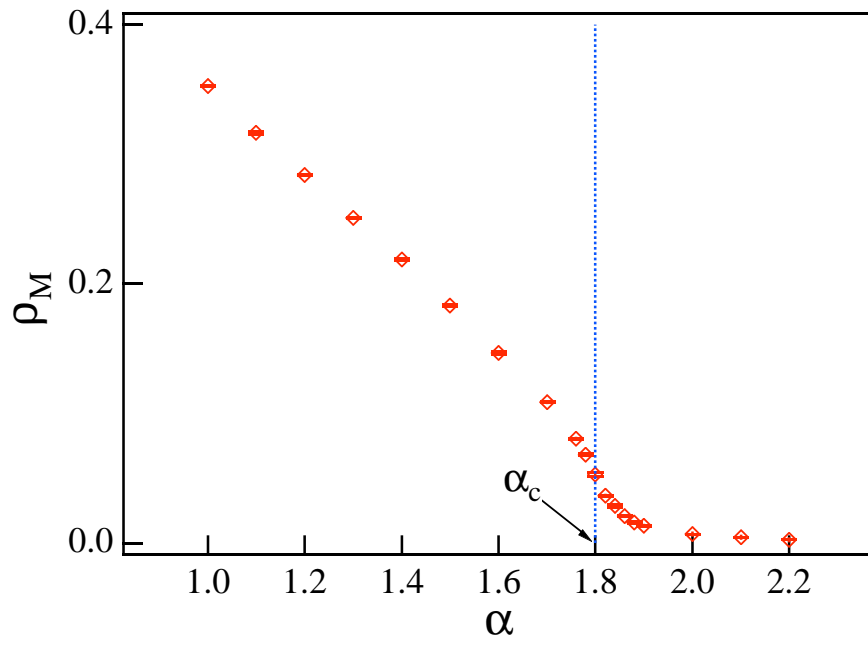


Fig.3

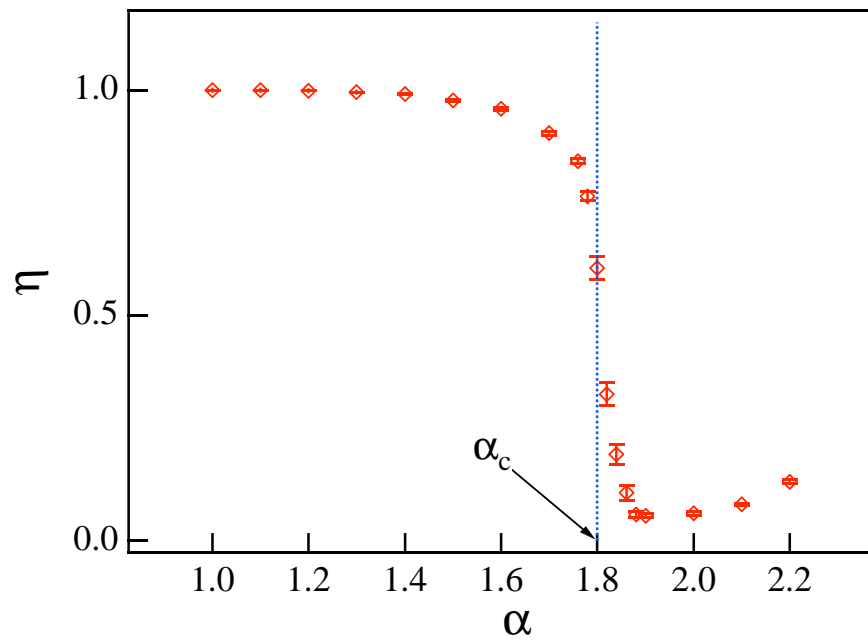


Fig.4



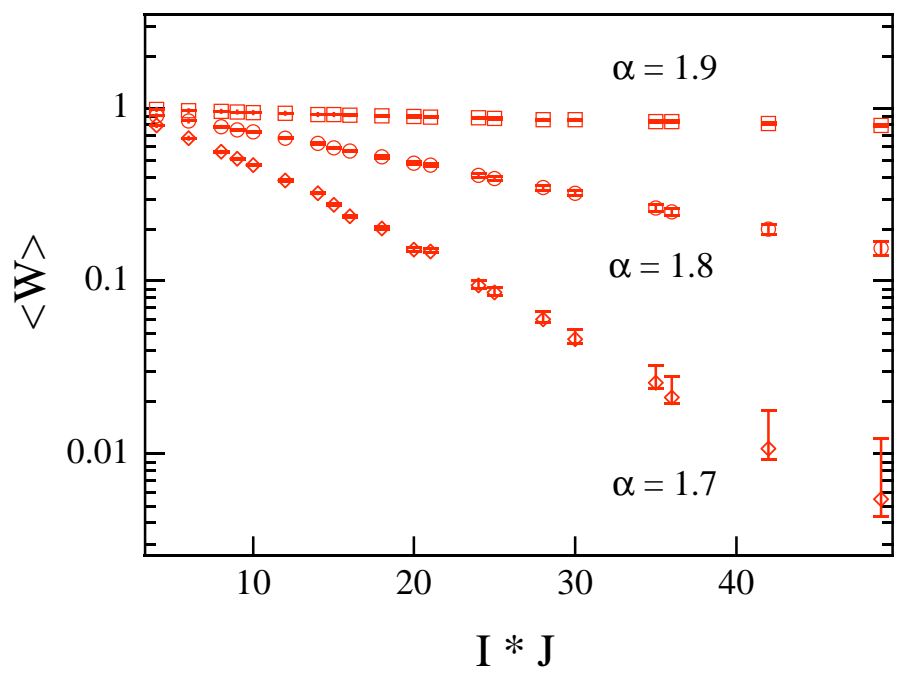


Fig.5

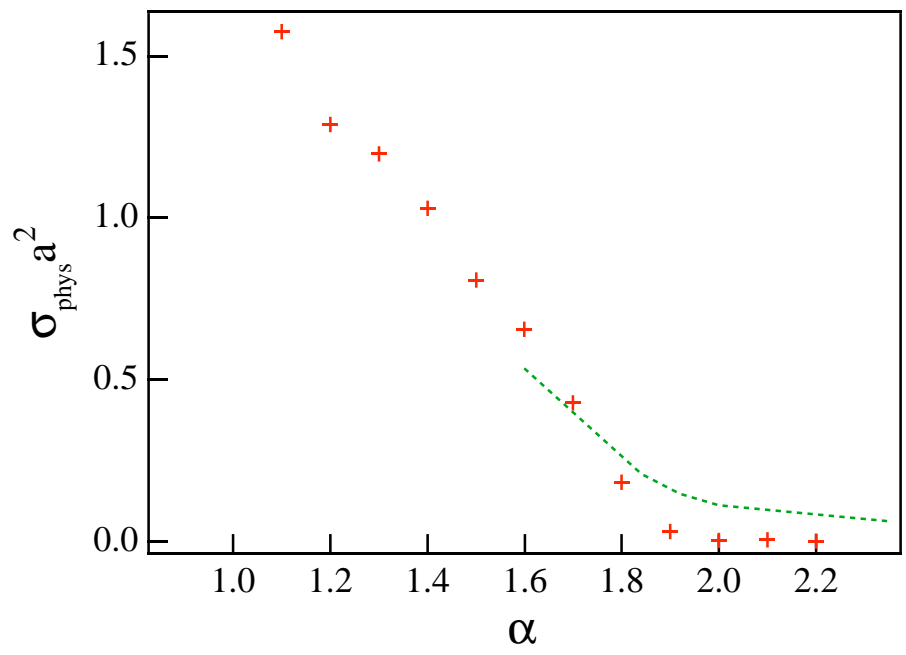


Fig.6